Combined Model of Photonucleon Reactions: Introduction in the Theory and Use of program Code

V. N. Orlin, K. A. Stopani*, V. V. Varlamov

Skobeltsyn Institute of Nuclear Physics, Lomonosov Moscow State University, Moscow, 119899 Russia

Abstract

A user manual describing the theory and operation of the computer code CMPNR (Combined Model of Photonucleon Reactions, or, equivalently, KMFR, from abbreviation of its name in Russian) is presented. This code, created at the Skobeltsyn Institute of Nuclear Physics (Moscow State University, Russia), combines into a single software package a number of theoretical works aimed at description of photonucleon reactions, published in last two decades. The CMPNR code is expected to be most useful at incident photon energies from the nucleon emission threshold to 50 MeV. The manual describes in detail the theoretical model, its computer implementation, the input parameters required to perform the computations, and the output data for typical problems. As an illustration, usage of CMPNR for evaluation of experimental cross sections of photonuclear reactions with different multiplicities is described.

PROGRAM SUMMARY/NEW VERSION PROGRAM SUMMARY

Program Title: Combined Model of Photonucleon Reactions

CPC Library link to program files: (to be added by Technical Editor)

Developer's repository link: `http://depni.sinp.msu.ru/~hatta/kmfr`

Licensing provisions: GPLv2

Programming language: Fortran

Supplementary material:

Nature of problem(approx. 50-250 words):

The purpose of the Combined model of photonucleon reactions is calculation of partial and total cross sections of photonuclear reactions on medium and heavy

*Corresponding author.

E-mail address: kstopani@sinp.msu.ru

nuclei in the energy range from the nucleon separation threshold to several tens of MeV. *Solution method(approx. 50-250 words):*
Additional comments including restrictions and unusual features (approx. 50-250 words):

---

1. Introduction

In the Combined Model of Photonucleon Reactions (CMPNR[1]), it is assumed that consideration of photonuclear reactions on β-stable medium and heavy nuclei ($A \gtrsim 25$–30 with $Z < 92$) at excitation energies of the target nucleus from the threshold of nucleon separation up to the threshold of π-meson production can be approximately limited to output reaction channels consisting of different combinations of emitted neutrons, protons and photons.

Up to the pion-production threshold, photoabsorption on a nucleus is determined by photon interaction only with one- and two-nucleon nuclear currents [1, 2]. In the first case, only single-nucleon excitations are formed after photon absorption. This is the dominant process in the region of low energies ($E_\gamma \lesssim 40$ MeV), where interaction of electromagnetic radiation with a nucleus leads to the formation of giant resonances which are collective bulk oscillations of nucleons. The quasideuteron (QD) photoabsorption mechanism becomes dominant above this region. Within this mechanism, the excited nucleon exchanges a virtual pion with the neighboring nucleon. As a result, the energy and momentum of the absorbed photon are transferred to a correlated proton-neutron pair rather than a single nucleon.

In describing giant resonances, use is most frequently made of various versions of the $1p1h$ approximation of the shell model — for example, the random phase approximation (RPA) [3], the theory of finite Fermi systems (TFFS) [4], and the coupled-channels method [5]. Despite the difference in substantiations, all of them lead to nearly identical results. For a reasonable choice of residual forces, these calculations reproduce by and large satisfactorily the mean energies and the sums of oscillator strengths of giant resonances in medium-mass and heavy nuclei. However, they run into serious difficulties in

[1]Transliterated abbreviation of the model's name in Russian is "KMFR", and it was referred to using this abbreviation during its development.

describing the structure and decay features of giant resonances. In the most advanced calculations of giant resonances, $2p2h$ states are therefore taken into account in addition to $1p1h$ configurations (see, for example, [6, 7, 8]). However, the problem of constructing a detailed description of the formation and decay of giant resonances has so far remained by and large unresolved because of limitations of the particle-hole approach. As a matter of fact, this approach can be used in describing giant resonances only in those cases where the ground state of the nucleus being considered does not differ very strongly from the particle-hole or quasiparticle physics vacuum. Therefore, it comes as no surprise that the most realistic microscopic calculations were performed for magic and nearly magic nuclei.

For this reason, a simple semimicroscopic approach [9, 10] is used in the CMPNR to describe giant resonances. This approach, supplemented with phenomenological data, makes it possible to describe the gross structure of giant resonances for the majority of medium-mass and heavy nuclei. The CMPNR also takes into account the isovector quadrupole resonance and the overtone of the giant dipole resonance which make a sizable contribution to photonucleon reactions in the energy range of 20–40 MeV. The quasi-deuteron component of the photoabsorption cross section in CMPNR is described using the Levinger quasi-deuteron model [11, 12].

In describing nucleon emission, which is the reaction stage following photoabsorption, one usually employs semiclassical statistical models (exciton [13-16] and hybrid [17-19] models) and quantum multistep preequilibrium models [20-22] combined with a evaporation model. Quantum models, in which the nucleon-emission probability is determined in terms of quantum-mechanical transition amplitudes, describe the angular distribution of reaction products better than semiclassical models. However, this drawback of semiclassical models is compensated to a considerable extent by the simplicity of their application and by their high predictive power in describing the nucleon energy spectra and partial photonucleon cross sections.

At the same time, the use of semiclassical preequilibrium models entails difficulties in describing photonuclear reactions at energies in the range of $E \lesssim 30$ MeV, because a powerful collectivized dipole state that arises as a coherent superposition of various 1p1h excitations appears to be the doorway state in this region. This circumstance is usually disregarded. However, this leads to serious errors in estimating the relative yields of photoneutrons and photoprotons and in describing their energy spectra.

In order to describe correctly the competition of the neutron and proton channels of the decay of a giant dipole resonance, it is necessary to take into account its isospin splitting into the $T_<$ and $T_>$ components, since, by virtue of isospin conservation, the $T_>$ component decays predominantly through the proton channel (in $N > Z$ nuclei) or through the neutron channel (in $N < Z$ nuclei). Without allowance for this circumstance, it is not possible to describe correctly the photonucleon yield either from comparatively light nuclei (of mass number in the range of $A \sim 25$–50), where the $T_>$ component of the giant dipole resonance is significant, or from heavy nuclei, where, despite the smallness of this component, it is an important source of photoprotons.

It should also be borne in mind that, within the preequlibrium models considered in [13-19], semidirect photonucleon reactions are treated as nucleon emission from the $1p1h$ doorway state. Concurrently, it is assumed that, at a given excitation energy, all $1p1h$ configurations are populated with equal probabilities, and the effect of the orbital angular (l) and total angular (j) momenta of an excited nucleon on its ability to leave the target nucleus is disregarded. This disregard of the shell structure of the doorway state leads to an incorrect consideration of the semi-direct photoelectric effect (the emission of an excited nucleon directly from the input state), which is especially important when describing the photodisintegration of light and medium nuclei, in which a significant proportion of photonucleons are emitted as a result of semi-direct reactions.

In the CMPNR, a correction of the semiclassical statistical model used at the stage of the reaction following the absorption of a photon was performed in order to take into account the influence of isospin effects and the collective nature of the doorway state for the GDR, which makes the main contribution to the emission of hard photonucleons at an energy of $E_\gamma \lesssim 40$ MeV.

2. Model Description

2.1. Photoabsorption cross section

Upon disregarding threshold effects, the total photoabsorption cross section can approximately be represented in the form

$$\sigma_{abs}(E_\gamma) \approx \sum_s \sigma_s(E_\gamma) \approx \sum_s \frac{2}{\pi} \frac{\sigma_{int}(s)\, E_\gamma^2\, \Gamma_s}{(E_\gamma^2 - E_s^2)^2 + E_\gamma^2 \Gamma_s^2} + \sigma_{QD}(E_\gamma), \qquad (1)$$

where the index s corresponds to components of the photoabsorption cross section, which are associated with various giant resonances (the dipole one, the isovector quadrupole one, and the overtone of the giant dipole resonance) which are approximated by one or several Lorentzian curves, depending on their structure, while the member $\sigma_{QD}(E_\gamma)$ describes the contribution of quasideuteron photoabsorption [11, 12].

For the resonance curves, the energies E_s and integrated cross sections $\sigma_{int}(s)$ are calculated on the basis of a semimicroscopic model of vibrations (see [9, 10]). In this case, the total integral photoabsorption cross-sections corresponding to various giant resonances are normalized using classical oscillatory sums multiplied by the factor $(1+\alpha) \approx 1.3$ in order to take into account the dependence of the nucleon-nucleon interaction on the nucleon momenta [23–25]. A isospin splitting of the resonance is taken into account only for GDR (in the case of medium nuclei according to the Fallieros et al. formulas [26, 27]), and a deformation splitting is taken into account only for the dipole and isovector quadrupole resonances. When calculating the deformation splitting of GDR, the results of the works [28, 29] are used. As calculations within the framework of the two-component nuclear liquid model [30, 31] show, the deformation splitting of GDR2 (overtone of GDR) with an error of less than 10% can be neglected, and for the isovector quadrupole resonance, the result shown in Fig. 1 is obtained.

The widths Γ_s included in the expression (1) are calculated using the exciton model. In the case of GDR, when calculating the values of E_s and Γ_s, the semi-empirical estimates of the average energy E_{dip} of GDR and the width of the spread $\Gamma^{\downarrow}_{dip}$ of this resonance over $2p2h$-states obtained in the work [32] are taken into account:

$$E_{dip} = 86\, A^{-1/3}\Theta^{-1}(a_0/R_0) \text{ MeV} \tag{2}$$

and

$$\Gamma^{\downarrow}_{dip} = 0.0293\, I(a_0/R_0)E^2 \text{ MeV}, \tag{3}$$

where

$$\Theta(a_0/r_0) = \left[\frac{1 + \frac{10}{3}\pi^2(a_0/r_0)^2 + \frac{7}{3}\pi^4(a_0/r_0)^4}{1+\pi^2(a_0/r_0)^2}\right]^{1/2} \tag{4}$$

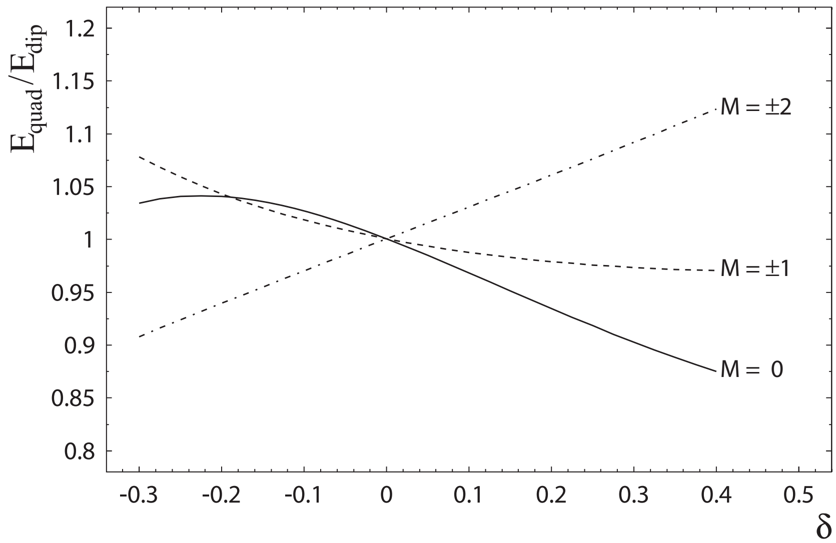

Figure 1: The dependence of the ratio of the energy E_{quad} of isovector quadrupole oscillations to the average energy E_{dip} of the giant dipole resonance (see relation 2.2) on the magnitude of the quadrupole deformation δ for different spherical components M of orbital angular momentum $L = 2$ of these oscillations.

and

$$I(a_0/R_0) = \frac{1}{1+\pi^2\left(\dfrac{a_0}{R_0}\right)^2}\left[1 - 3\frac{a_0}{R_0}\frac{1+\dfrac{\pi^2}{3}\left(\dfrac{a_0}{R_0}\right)^2}{1+\pi^2\left(\dfrac{a_0}{R_0}\right)^2}\right] \qquad (5)$$

are factors that take into account the diffuseness of the nuclear surface, a_0 and R_0 are the parameters of the radial Fermi form factor for the charge distribution in the nucleus ($a_0 \approx 0.55$ fm, $R_0 \approx 1.07A^{1/3}$ fm).

2.2. Decay of doorway states: a general approach

In the exciton model, it is assumed that, after photon absorption, there arises a doorway state featuring $m = m_0$ excitons ($m_0 = 2$ for giant resonances that are $1p1h$-excitations, and $m_0 = 4$ for a quasideuteron $2p2h$-excitation). This primary excitation decays via excited-nucleon emission

($m \to m-1$ transition), photon emission, or (what is more probable) an $m \to m+2$ transition leading to a more complicate particle-hole configuration and occurring under the effect of residual two-body interaction. After that, the same occurs once again. The new exciton state formed at the preceding step either emits a nucleon or a photon to a continuum or undergoes an $m \to m+2$ intranuclear transition, and so on. As the result of ($m \to m+2$) intranuclear transitions, the excitation energy of the composite system is distributed among an ever greater number of excitons. At the same time, $m \to m-2$ inverse transitions caused by the annihilation of one of the particle-hole pairs because of the transfer of its energy to some particle or hole are also possible. These transitions play a minor role as long as the total number of particles and holes in the system is moderately small. As their number increases, the probability of such transitions gradually grows and ultimately becomes equal to the probability of direct transitions. At this instant, the system reaches the state of thermal equilibrium either in the primary nucleus or in one of the residual nuclei, whereupon a comparatively long nucleon-evaporation process accompanied by photon emission begins. This process can be described on the basis of the evaporation model. Preequilibrium nucleon emission becomes extinct long before equilibration (as early as the first reaction stages); therefore, in the CMPNR reverse transitions are ignored.

Because of nucleon and photon emission, the chain of doorway-state decays ends up in the formation of some final nucleus $\{Z_{fin}, N_{fin}\}$ in the ground state. In order to trace all details of occurring processes, in the CMPNR the energy spectrum of excitations of the composite system is discretized with a step $\Delta E = 0.2$ MeV and the resulting energy bands are treated as discrete levels of nuclei with energies $E_1 = E_\gamma > E_2 > \ldots > E_N = 0$. Then the probabilities $P(n_\pi, n_\nu, m, E_i, [T])$ and $P(n_\pi, n_\nu, E_i, [T])$ of population of m-exciton states $|n_\pi, n_\nu, m, E_i, [T]\rangle$ and equilibrium states $|n_\pi, n_\nu, E_i, [T]\rangle$, $i = 1, 2, \ldots, N$ during decay of the input state $|n_\pi = 0, n_\nu = 0, m_0, E_1, [T_0]\rangle$ are calculated. Here the numbers n_π and n_i indicating how many protons and neutrons, respectively, escaped from the $\{Z, N\}$ target nucleus before the emergence of a $\{Z', N'\} = \{Z - n_\pi, N - n_\nu\}$ intermediate nucleus (the total number of emitted nucleons is $n = n_\pi + n_\nu$); T is the isospin of the corresponding exciton or equilibrium state. The isospin T is taken into account only in the decay of the GDR; therefore, it is bracketed as an optional argument.

It should also be noted that when describing the decay of GDR for each intermediate nucleus $\{Z', N'\}$ one can limit oneself to only two values of isospin T: T_0' and $T_0'+1$, where $T_0' = |(N'-Z')/2|$ is the ground-state isospin of this nucleus, since the GDR lies at comparatively low excitation energies (not higher than 30 MeV), and this substantially simplifies the problem of taking into account isospin effects.

The decay of an arbitrary doorway state is schematically depicted in Fig. 1, where, by $|n, m\rangle$ and $|n\rangle$, one mean the m-exciton states $|n_\pi, n_\nu, m, E, [T]\rangle$ and and the equilibrium states $|n_\pi, n_\nu, E, [T]\rangle$ and where $E_{max}(n) \equiv E_{max}(n_\pi, n_\nu) = E_\gamma - [n_\pi\, m_{prot} + n_\nu\, m_{neutr} + M(Z-n_\pi, N-n_\nu) - M(Z,N)]c^2$ is the maximum excitation energy when the evolution of a composite system leads to the formation of a nucleus $\{Z-n_\pi, N-n_\nu\}$.

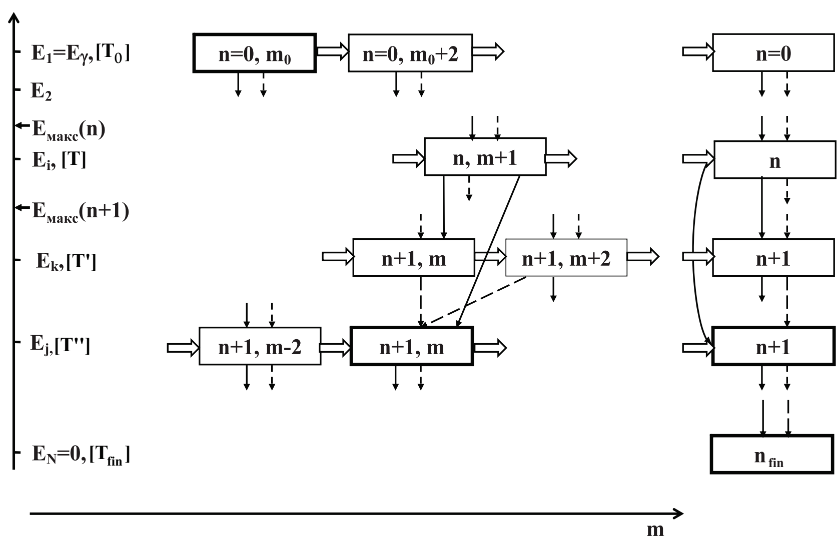

Figure 2: Scheme of a photonucleon reaction after the formation a doorway state. The solid-line, dashed-line, and double arrows indicate, respectively, nucleon emission, photon emission, and intranuclear transitions leading to the production of yet another particle-hole pair.

The occupation probability for the m-exciton state $|n_\pi, n_\nu, m, E_i, [T]\rangle$ ($i = 1, 2, \ldots N$) is equal to the sum of the probabilities for the transitions to it from states that appeared at earlier reaction stages; that is [25],

$$
\begin{aligned}
&P\left(n_\pi, n_\nu, m, E_i, [T]\right) = \hbar\Delta E \sum_{k=\pi,\nu} \sum_{[T']} \sum_{E_i<E_j\le E_{max}(n'_\pi,n'_\nu)} P(n'_\pi, n'_\nu, m{+}1, E_j, [T']) \times \\
&\times\ \lambda_k(n'_\pi, n'_\nu, m{+}1, E_j{-}E_i{-}B'_k, E_j, [T'] \to [T])/\Gamma(n'_\pi, n'_\nu, m{+}1, E_j, [T']) + \\
&+\ \hbar\Delta E \sum_{[T']} \sum_{E_i<E_j\le E_{max}(n_\pi,n_\nu)} P(n_\pi, n_\nu, m, E_j, [T']) \times \\
&\times\ \lambda_\gamma^{(1)}(n_\pi, n_\nu, m, E_j{-}E_i, E_j, [T'] \to [T])/\Gamma(n_\pi, n_\nu, m, E_j, [T']) + \\
&+\ \hbar\Delta E \sum_{[T']} \sum_{E_i<E_j\le E_{max}(n_\pi,n_\nu)} P(n_\pi, n_\nu, m{+}1, E_j, [T']) \times \\
&\times\ \lambda_\gamma^{(2)}(n_\pi, n_\nu, m{+}1, E_j{-}E_i, E_j, [T'] \to [T])/\Gamma(n_\pi, n_\nu, m{+}1, E_j, [T']) + \\
&+\ P(n_\pi, n_\nu, m{-}2, E_i, [T])\Gamma^{\downarrow}(n_\pi, n_\nu, m, E_i, [T])/\Gamma(n_\pi, n_\nu, m, E_i, [T]), \qquad (6)
\end{aligned}
$$

where $n'_\pi = n_\pi - \delta_{k\pi}$, $n'_\nu = n_\nu - \delta_{k\nu}$, B'_k is the separation energy for a nucleon of type k (a proton or a neutron) from the $\{Z - n'_\pi, N - n'_\nu\}$ nucleus; $\lambda_k(n'_\pi, n'_\nu, m+1, \varepsilon, E, [T'] \to [T])$ is the rate of the $(T' \to T)$ decay of the state $|n'_\pi, n'_\nu, m{+}1, E, [T']\rangle$ with the emission of a k-type nucleon of energy ε to a continuum; $\Gamma(n_\pi, n_\nu, m, E, [T])$ is the total width of the state $|n_\pi, n_\nu, m, E, [T]\rangle$; $\Gamma^{\downarrow}(n_\pi, n_\nu, m, E, [T])$ is that component of this width which is due to intranuclear transitions; and $\lambda_\gamma^{(1)}(n_\pi, n_\nu, m, \varepsilon, E, [T'] \to [T])$ and $\lambda_\gamma^{(2)}(n_\pi, n_\nu, m, \varepsilon, E, [T'] \to [T])$ are the components of the rate of m-exciton state decay occurring via photon emission, respectively, without and with a change in the number of excitons $[\lambda_\gamma(\ldots) = \lambda_\gamma^{(1)}(\ldots) + \lambda_\gamma^{(2)}(\ldots)$ is the total rate of decay of this state via photon emission$]$.

An expression for the population of the equilibrium state $|n_\pi, n_\nu, E_i, [T]\rangle$ $(i = 1, 2, \ldots .N)$ can be obtained in a similar way:

$$
\begin{aligned}
&P\left(n_\pi, n_\nu, E_i, [T]\right) = P(n_\pi, n_\nu, m_{meam}, E_i, [T]) + \\
&+\ \hbar\Delta E \sum_{k=\pi,\nu} \sum_{[T']} \sum_{E_i<E_j\le E_{max}(n'_\pi,n'_\nu)} P(n'_\pi, n'_\nu, E_j, [T']) \times \\
&\times\ \lambda_j(n'_\pi, n'_\nu, E_j{-}E_i{-}B'_k, E_j, [T'] \to [T])/\Gamma(n'_\pi, n'_\nu, E_j, [T']) + \\
&+\ \hbar\Delta E \sum_{[T']} \sum_{E_i<E_j\le E_{max}(n_\pi,n_\nu)} P(n_\pi, n_\nu, E_j, [T']) \times \\
&\times\ \lambda_\gamma(n_\pi, n_\nu, E_j{-}E_i, E_j, [T'] \to [T])/\Gamma(n_\pi, n_\nu, E_j, [T']), \qquad (7)
\end{aligned}
$$

where $m_{mean} = 0.8(aE_i)^{1/2}$ is the mean number of excitons in the equilibrium state ($a \approx 0.047A$ MeV^{-1} is the level-density parameter); the rest of the notations are obvious — compare with the notations in the formula (6).

In calculating the quantities λ_k, $\lambda_\gamma^{(1)}$, $\lambda_\gamma^{(2)}$, Γ and $\Gamma^{\downarrow}$ included in equation (2.6), we used the densities of exciton states found within the Fermi gas model using the procedure described in Ref. [33]. The characteristics of the decay of equilibrium states appearing in equation (7) were calculated using the level densities following from the Global models (see [34]). The influence of isospin effects on the decay rate of exciton and equilibrium states is discussed in the next subsection (see also [25]).

The recursion relations (6) and (**??**) make it possible to calculate the whole chain of occupation probabilities for exciton and equilibrium states of the composite system since $P(n_\pi = 0, n_\nu = 0, m = m_0, E_1, [T_0]) = 1$ and $P(n_\pi = 0, n_\nu = 0, E_1, [T_0]) = P(n_\pi = 0, n_\nu = 0, m = m_{mean}, E_1, [T_0])$.

Knowing all of these probabilities, one can readily calculate the partial photonucleon reaction cross sections corresponding to the emission of specific numbers of protons and neutrons from the target nucleus and the photonucleon energy spectra integrated with respect to the emission angle.

For example, the partial photonucleon reaction cross section $\sigma(n_\pi, n_\nu, E_\gamma)$ is obviously given by the expression

$$\sigma(n_\pi, n_\nu, E_\gamma) = \sum_s \sigma_s(E_\gamma) P_s(n_\pi, n_\nu, E_N = 0, [T_{fin}]), \tag{8}$$

where summation is performed over all components of the photonucleon reaction cross section [see expression (1)] to each of which its own doorway state $|s\rangle$ corresponds and $T_{fin} = |(N - Z - n_\nu + n_\pi)/2|$ is the ground-state isospin of the final nucleus. The photoproton and photoneutron energy spectra integrated with respect to the emission angle can be calculated by the formula

$$\begin{aligned}\frac{d\sigma_k(\varepsilon, E_\gamma)}{d\varepsilon} &= \hbar \sum_s \sigma_s(E_\gamma) \sum_{n_\pi} \sum_{n_\nu} \sum_{[T]} \sum_{[T']} \sum_{B_k < E_j \le E_{max}(n_\pi, n_\nu)} \Bigg\{ P_s(n_\pi, n_\nu, E_j, [T]) \times \\ &\times \lambda_k^{(s)}(n_\pi, n_\nu, \varepsilon, E_j, [T] \to [T']) / \Gamma^{(s)}(n_\pi, n_\nu, E_j, [T]) + \\ &+ \sum_{m=m_0}^{m_{mean}-1} P_s(n_\pi, n_\nu, m, E_j, [T]) \lambda_k^{(s)}(n_\pi, n_\nu, m, \varepsilon, E_j, [T] \to [T']) \times \\ &\times [\Gamma^{(s)}(n_\pi, n_\nu, m, E_j, [T])]^{-1} \Bigg\},\end{aligned} \tag{9}$$

where $k = \pi$ and $k = \nu$ for protons and neutrons, respectively.

2.3. Isospin effects

As noted in the Introduction, when considering photonucleon reactions in the GDR region, it is important to take into account isospin effects. In estimating the decay features $\lambda_k(m, \varepsilon, E)$ and $\lambda_k(\varepsilon, E)$ $(k = \pi, \nu)$ of exciton and equilibrium states on the basis of semiclassical statistical models [13-19], these effects are disregarded, which leads to a catastrophic underestimation of the photoproton yield in medium-mass nuclei.

Meanwhile, it is not difficult to take these effects into account in calculating such features. In the following, in order to avoid duplication of the same reasoning, the formulas describing the preequilibrium and equilibrium emission of photonucleons are combined, for which the number of excitons m is enclosed in square brackets. It implies that this argument is used only at the preequilibrium stage of the reaction.

Let a group A of states $|[m], E, T\rangle$ of some initial nucleus with isospin $T = T_0, T_0 + 1$, which are located in the energy interval $E \pm \Delta E/2$, decays due to the emission of a nucleon of type $k = \pi, \nu$ (a proton or a neutron) with energy $\varepsilon \pm d\varepsilon/2$ into states of the composite system B, including the states of the final nucleus $|[m-1], E', T'\rangle$ in the energy interval $E' = E - B_k - \varepsilon \pm \Delta E/2$ with isospin $T' = T'_0, T'_0 + 1$ plus the states of the emitted nucleon (B_k is the separation energy of a nucleon of type k, T_0 and T'_0 are the isospins of the initial and final nuclei in the ground state).

According to the detaile-dbalance principle, the probabilities $P_k(A \to B)$ and $P_k(B \to A)$ for the transitions from A to group B and from group B to group A, respectively, then satisfy the relation

$$\frac{P_k(A \to B)}{\mathrm{g}_B} = \frac{P_k(B \to A)}{\mathrm{g}_A}\,, \tag{10}$$

where $\mathrm{g}_A = \omega([m], E, T)\,\Delta E$ is the statistical weight of states of group A; $\mathrm{g}_B = \omega([m-1], E', T')\rho_{fre}(\varepsilon)\,\Delta E\,d\varepsilon$ is the statistical weight of states of group B; $\omega([m], E, T)$ and $\omega([m–1], E', T')$ are the densities of states in, respectively, the initial and the final nucleus at the respective energies; and

$$\rho_{fre}(\varepsilon) = \frac{V(2s+1)}{2\pi^2\hbar^3}\sqrt{2\mu^3\varepsilon} \tag{11}$$

is the density of states for a free nucleon lying in the volume V (here, $s = 1/2$ is the spin of the nucleon and μ is its reduced mass).

The probability for the inverse transition $B \to A$ can be represented as the product of three factors; that is,

$$P_k(B \to A) = V^{-1}\sqrt{\frac{2\varepsilon}{\mu}}\,\sigma_k^{inv}(\varepsilon) \times \frac{\omega([m],E,T)}{\omega([m],E)} \times f_{B,A}(T' \to T). \qquad (12)$$

Here, the first factor determines the probability for the inverse process (nucleon capture by the final nucleus) in the case where the states does not differ in isospin either in the initial or in the final nucleus. The inverse-reaction cross section

$$\sigma_k^{inv}(\varepsilon) = \frac{1}{2}\pi\lambda\!\!\!^{-2}\sum_{jl}(2j+1)T_{jl}^k(\varepsilon), \qquad (13)$$

where T_{jl}^k is the transmission coefficient for a nucleon belonging to type k and having an orbital angular momentum l and a total angular momentum j, can be calculated on the basis of the optical model. The second factor takes into account the circumstance that, in the initial nucleus, we are interested in the population of only those states that have a fixed isospin, $T = T_0$ or $T_0 + 1$ ($\omega([m],E) = \omega([m],E,T_0) + \omega([m],E,T_0+1)$ is the total density of states in the initial nucleus at the energy E). The last, third, factor characterizes the probability of the transition $T \to T'$ upon absorption of a photon by a nucleus in a state with excitation energy E'. Since the probability of this event is proportional to the product of the density of states $|[m-1],E',T'\rangle$ and the square of the respective Clebsch-Gordan coefficient, the factor $f_{B,A}(T' \to T)$ can obviously be represented in the form

$$\begin{aligned} f_{B,A}(T' \to T) = {} & \omega([m-1],E',T')(T'T_{0z} - t_{zk}\,\frac{1}{2}t_{zk}|TT_{0z})^2 \times \\ & \times\Bigg(\omega([m-1],E',T_0')(T_0'T_{0z} - t_{zk}\,\frac{1}{2}t_{zk}|TT_{0z})^2 + \\ & + \omega([m-1],E',T_0'+1)(T_0'+1T_{0z} - t_{zk}\,\frac{1}{2}t_{zk}|TT_{0z})^2\Bigg)^{-1}, \end{aligned} \qquad (14)$$

where $T_{0z} = (N-Z)/2$ is the z projection of the initial-nucleus isospin and t_{zk} is the z projection of the emitted-nucleon isospin.

From Eqs. (10)–(12), it follows that the rate of decay of the initial-nucleus state $|[m],E,T\rangle$ to the final-nucleus state $|[m-1],E',T'\rangle$ via the emission of a k-type nucleon with energy ε is

$$\begin{aligned}\lambda_k([m],\varepsilon,E,T\to T') = P_k(A\to B)/d\varepsilon = \\ = \frac{2s+1}{\pi^2\hbar^3}\,\mu\varepsilon\sigma_k^{inv}(\varepsilon)\frac{\omega([m-1];E',T')}{\omega([m],E)}f_{B,A}(T'\to T),\end{aligned} \qquad (15)$$

where the factor $f_{B,A}(T'\to T)$ is given be expression (14).

In medium-mass and heavy nuclei, $\omega([m-1],E',T'_0)\approx\omega([m-1],E')\gg\omega([m-1],E',T'_0+1)$ and $f_{B,A}(T'_0\to T_0)\approx 1$ in the energy region being considered; therefore, can disregard transitions to $T'=T'_0+1$ final-nucleus states in describing the decay features of the $T_<$ giant-dipole-resonance component. Formula (15) then transforms into the standard formula of the statistical model [13].

In the decay of the $T_>$ giant-dipole-resonance component via proton emission, the situation is similar, since this decay proceeds predominantly to the T'_0-states of the final nucleus. In the decay of the $T_>$ component of the GDR via neutron emission, only the (T'_0+1) states of the final state are available (in this case $f_{B,A}(T'_0+1\to T_0+1)=1$). The rate of such decay, proportional to $\omega([m-1],E',T'_0+1)$, is significantly less than the rate of decay via proton emission $\lambda_\pi([m],\varepsilon,E,T_0+1\to T'_0)\propto\omega([m-1],E',T'_0)$. This explains the predominant emission of protons during the decay of the $T_>$ component of the GDR.

The densities of final states in massive nuclei can be approximated by the expressions

$$\begin{aligned}\omega([m-1],E',T'_0) &\approx \omega([m-1],E'),\\ \omega([m-1],E',T'_0+1) &\approx \begin{cases}\omega([m-1],E'-\Delta'_1) \text{ for } E'\geq\Delta'_1,\\ 0 \text{ for } E'<\Delta'_1,\end{cases}\end{aligned} \qquad (16)$$

where Δ'_1 is the energy of the first excited level with isospin T'_0+1 in the final nucleus.

In lighter nuclei ($A<50$), it is necessary to take into account both branches of T transitions described by expression (15). It is also necessary to refine the estimates of the densities of final states characterized by various values of the isospin quantum number. We represent these densities of states in the form

$$\begin{aligned}\omega([m-1],E',T'_0) &\approx \omega([m-1],E')\frac{1}{1+q(E')}\,,\\ \omega([m-1],E',T'_0+1) &\approx \omega([m-1],E')\frac{q(E')}{1+q(E')}\,,\end{aligned} \qquad (17)$$

where

$$q(E') \approx \begin{cases} \omega([m-1], E' - \Delta_1')/\omega([m-1], E') \text{ for } E' \geq \Delta_1', \\ 0 \text{ for } E' < \Delta_1', \end{cases} \tag{18}$$

For $q(E') \to 0$, the estimates in (17) go over to the estimates in (16). Moreover, they satisfy the relation $\omega([m-1], E') = \omega([m-1], E', T_0') + \omega([m-1], E', T_0' + 1)$.

2.4. Photon decay channel

At low excitation energies ($E < 30$ MeV), electromagnetic transitions in medium and heavy nuclei satisfy the isospin selection rules $\Delta T = -1, 0, 1$, $\Delta T_z = 0$. Therefore, the photon emitted or absorbed in such a transition can be considered as a particle with isospin quantum numbers $t = 1$ and $t_z = 0$. This allows us to obtain, using the principle of detailed balance, an expression for the rate of photon emission from the pre-equilibrium (or equilibrium) state $|[m], E, T\rangle$ of the nucleus $\{N, Z\}$ similar to the expression (15):

$$\begin{aligned} \lambda_\gamma^{(k)}([m], \varepsilon_\gamma, E, T \to T') = \frac{\varepsilon_\gamma^2}{\pi^2 c^2 \hbar^3} \, \sigma_{abs}(\varepsilon_\gamma) \times \\ \times \frac{\omega([m-2\delta_{k2}]; E', T')}{\omega([m], E)} \hat{f}_{BA}^{(k)}(T' \to T), \end{aligned} \tag{19}$$

where $k = 1, 2$; E, T and E', T' are the energy and isospin of the initial and final states of the nucleus $\{N, Z\}$, respectively; $\varepsilon_\gamma = E - E'$ is the energy of the emitted photon, $\sigma_{abs}(\varepsilon_\gamma)$ is the photoabsorption cross section on the nucleus $\{N, Z\}$ and

$$\begin{aligned} \hat{f}_{B,A}^{(k)}(T' \to T) = \omega([m-2\delta_{k2}], E', T')(T' T_{0z}\, 10|T T_{0z})^2 \times \\ \times \Big(\omega([m-2\delta_{k2}], E', T_0)(T_0 T_{0z}\, 10|T T_{0z})^2 + \\ + \omega([m-2\delta_{k2}], E', T_0+1)(T_0+1 T_{0z}\, 10|T T_{0z})^2 \Big)^{-1} \end{aligned} \tag{20}$$

a factor characterizing the probability of the transition $T \to T'$ upon absorption of a photon by a nucleus in a state with excitation energy E'.

($T_0 = |T_{0z}| = |(N-Z)/2|$ is isospin of the ground state of the nucleus $\{N, Z\}$).

At higher energies, above GDR, for medium and heavy nuclei, isospin effects can be neglected due to their smallness. Therefore, when describing the emission of photons during the decay of isovector quadrupole resonance, GDR overtone and quasi-deuteron excitations, the total densities of exciton (or equilibrium) states and the factor $\hat{f}^{(k)}_{B,A} = 1$ are substituted into the formula (19).

2.5. Influence of coherence of doorway dipole state

In the shell model, the doorway-dipole state of an axisymmetric nucleus is treated as a coherent superposition of $1p1h$ states, $|\alpha, \beta^{-1}\rangle$, where $|\alpha\rangle = \sum\limits_{lj\in\alpha} c_{lj}|nljm\rangle$ and $|\beta\rangle$ are single-particle states having a specific value of the projection m of the angular momentum onto the symmetry axis of the nucleus and corresponding, for example, to the Nilsson potential ($|nljm\rangle$ are eigenstates of a spherical harmonic oscillator).

For the doorway dipole state at an energy E, the rate of decay accompanied by the emission of a nucleon with energy ε from the nucleus can be represented in the form

$$\lambda_{dip}(\varepsilon, E) = \sum_{\alpha\beta^{-1}} P_{\alpha\beta^{-1}} \sum_{lj\in\alpha} c^2_{lj}\, \lambda(\alpha\beta^{-1}, E; \varepsilon ljm), \tag{21}$$

where $P_{\alpha\beta^{-1}}$ is the relative probability for the dipole excitation of the configuration $|\alpha\beta^{-1}\rangle$ [it is proportional to the squared matrix element of the single-particle $E1$ transition: $\langle\alpha|2t_z r Y_{1M}(\hat{\mathbf{r}})|\beta\rangle^{\mathbf{2}}$, the sum of such probabilities for all nucleon transitions of the same type must be equal to unity],

$$\lambda(\alpha\beta^{-1}, E; \varepsilon ljm) = \frac{2s+1}{\pi^2\hbar^3}\, \mu\varepsilon\, \sigma^{inv}_{ljm}(\varepsilon)\, \frac{\omega(\beta^{-1}, E')}{\omega(\beta^{-1}, ljm; E)} \tag{22}$$

is the probability for the decay per unit time of the configuration $|\alpha\beta^{-1}, E\rangle$ with the emission of a εljm-nucleon, $\sigma^{inv}_{ljm}(\varepsilon) = \frac{1}{2}\pi\lambda\!\!\!^{-2} T_{jl}(\varepsilon)$ is the cross section for the absorption of a εljm-nucleon, $\omega(\beta^{-1}, E')$ is the distribution density for a hole β^{-1} in the vicinity of the energy $\varepsilon_{\beta^{-1}}$ ($E' = E - B_{thr} - \varepsilon$),

$$\omega(\beta^{-1}, ljm; E) = \int\limits_0^{E-B_{thr}} \omega_{ljm}(\varepsilon)\, \omega(\beta^{-1}, E - B_{thr} - \varepsilon)\, d\varepsilon \tag{23}$$

is the total density of the configurations $|\beta^{-1}, ljm\rangle$ at the energy E that have preset quantum numbers $\{\beta ljm\}$, and $\omega_{ljm}(\varepsilon)$ is the total density of ljm-states to which a nucleon of energy ε can be captured.

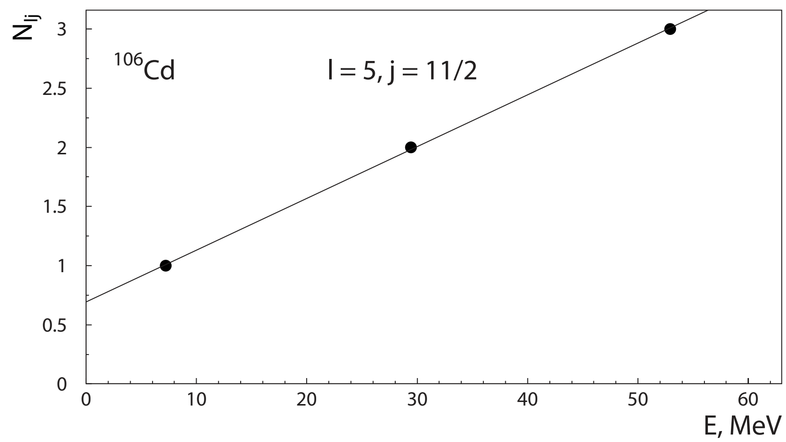

Figure 3: Change in the number of ljm-levels in the ^{106}Cd (closed circles) as the excitation energy grows.

Figure 3 shows a typical picture of how, in the Nilsson spherical potential, the number of single-particle levels that have fixed quantum numbers ljm changes as the particle excitation energy grows. From this figure, one can see that the number of such states grows with energy linearly: $N_{lj} = a_{lj} + \mathrm{g}_{lj}\,\varepsilon$. Therefore, the single-particle level densities $\omega_{ljm}(\varepsilon) = d\,[N_{lj}(\varepsilon)]/d\varepsilon$ can be approximated by the constants g_{lj} found in this way. The hole-distribution density $\omega(\beta^{-1}, E')$ appearing in expressions (22) and (23) can be approximated by a Breit-Wigner curve normalized to unity in the range of $0 \leq E' \leq \infty$, its width being estimated on the basis of the optical model.

In [23], the $T_<$ and $T_>$ components of the giant dipole resonance were separated within the semimicroscopic model of vibrations that was proposed in [9, 37]. If the spread of the energies of single-particle transitions and pair correlations in the $|T_0, T_{0z}\rangle$ ground state of the nucleus are disregarded, then the wave functions for the $T_<$ and $T_>$ dipole states can approximately be represented in the form

$$
\begin{aligned}
|\Psi_{1M}(T_0{+}1,T_{0Z})\rangle &= C_{>}\sum_{\alpha\in\{\alpha_n\}}\sum_{\beta\in\{\beta_p\}}\langle\alpha|2t_z rY_{1M}(\hat{\mathbf{r}})|\beta\rangle a^+_\alpha a_\beta|T_0,T_{0Z}\rangle,\\
|\Psi_{1M}(T_0,T_{0Z})\rangle &= C_{<}\Bigg[\sum_{\alpha}\sum_{\beta}\langle\alpha|2t_z rY_{1M}(\hat{\mathbf{r}})|\beta\rangle a^+_\alpha a_\beta -\\
&\quad -\frac{1}{T_0{+}1}\sum_{\alpha\in\{\alpha_n\}}\sum_{\beta\in\{\beta_p\}}\langle\alpha|2t_z rY_{1M}(\hat{\mathbf{r}})|\beta\rangle a^+_\alpha a_\beta\Bigg]|T_0,T_{0Z}\rangle,
\end{aligned}
\tag{24}
$$

where summation $\sum\limits_{\alpha\in\{\alpha_n\}}\sum\limits_{\beta\in\{\beta_p\}}$ is performed only over single-particle neutron and proton transitions that proceed between levels occupied in protons and levels vacant for neutrons and where $C_{>}$ and $C_{<}$ are normalization constants.

Relations (24) make it possible to estimate the decay features of doorway states for the $T_{<}$ and $T_{>}$ components of the giant dipole resonance individually. These relations were obtained under the assumption that the target nucleus is neutron-rich. If this is not so, it is necessary to make the substitutions $\{\alpha_n\}\to\{\alpha_p\}$ and $\{\beta_p\}\to\{\beta_n\}$ in them.

2.6. The place of CMPNR among other nuclear reaction codes

Unlike such frequently used programs as TALYS and EMPIRE, which attempt to statistically describe various nuclear reactions in a wide mass range, CMPNR considers only photonucleon reactions on β-stable medium ($A \gtrsim$ 25-30) and heavy (below transuranic elements) nuclei with a sufficiently hard surface in the range of incident photon energies from the nucleon emission threshold to the π-meson production threshold. This is a specialized program designed to describe the nuclear photoelectric effect in cases where the emission of particles other than neutrons, protons and photons from an excited nucleus can be neglected, which significantly simplifies the solution of the problem under consideration.

The narrowing of the scope of applicability of the program is largely compensated by taking into account a number of important effects influencing the competition of neutron and proton reaction channels, which are not considered in more universal codes. Thus, in the CMPNR, the conservation of isospin is taken into account both at the stage of GDR formation, which makes the main contribution to the photoabsorption cross section at $E_\gamma \lesssim 30$ MeV, and at the stage of its decay, which significantly affects the ratio of neutron and proton yields, especially for nuclei with $A \lesssim$ 50-60, since the $T_>$ component of GDR decays mainly with proton emission. In addition, the CMPNR takes into account the fact that the doorway dipole state is in fact a coherent superposition of 1p1h states, which, as calculations show, increases the share of high-energy particles in the energy spectrum of photonucleons. This also contributes to an increase in the yield of protons, since, having a high energy, they more easily overcome the Coulomb barrier. The influence of these two factors on photonucleon reactions is illustrated in Figs. 4-6.

In Fig. 4, a comparison is made of the experimental cross sections of the reactions ^{64}Zn(γ, n) + ^{64}Zn$(\gamma, n+p)$ and ^{64}Zn$(\gamma, 2n)$ + ^{64}Zn$(\gamma, 2n+p)$ [38] with the results of calculations of these cross sections, performed within the framework of the CMPNR model taking into account (Figs. 4a and 4b) and without taking into account (Figs. 4c and 4d) the influence of isospin effects and collectivization of the doorway state during dipole photoabsorption.

As can be seen from Fig. 4, neglecting the collective properties and isospin effects in describing the GDR decay leads to an inadequately large photoneutron yield compared to the experimental data. This is mainly due to the fact that disregarding the isospin selection rules removes the prohibition of the neutron decay of the $T_>$ component of the GDR to states with the minimum isospin of the final nucleus (compare the behavior of the red curves in Fig. 4a, b and 4c, d).

The necessity of taking into account at least isospin effects when describing photonucleon reactions on medium and medium-heavy nuclei is also confirmed by photoproton experimental data. In Fig. 5, the experimental data for the cross section of the ^{90}Zr(g, p) reaction [39, 40, 41] are compared with the results of calculations of this cross section, performed: a) taking into account both the isospin selection rules during the decay of the GDR and the collective properties of the doorway dipole state, b) taking into account only isospin effects, and c) without taking into account both of these factors.

As follows from the data presented in Fig. 5, neglect of the collective properties of the doorway dipole state leads to some decrease in the theoretical cross section of the ^{90}Zr(γ, p) reaction. However, this decrease is comparatively small, since the effect of the collectivization of the doorway state extends only to the pre-equilibrium stage of the reaction, while the bulk of photoprotons are emitted during evaporation. It is a different matter when isospin effects are not taken into account. In this case, the theory (see Fig. 4c) is unable to explain the existence of a broad peak in the cross section of the reaction under consideration at an energy of $E_\gamma \approx 21$ MeV, since the $T_>$

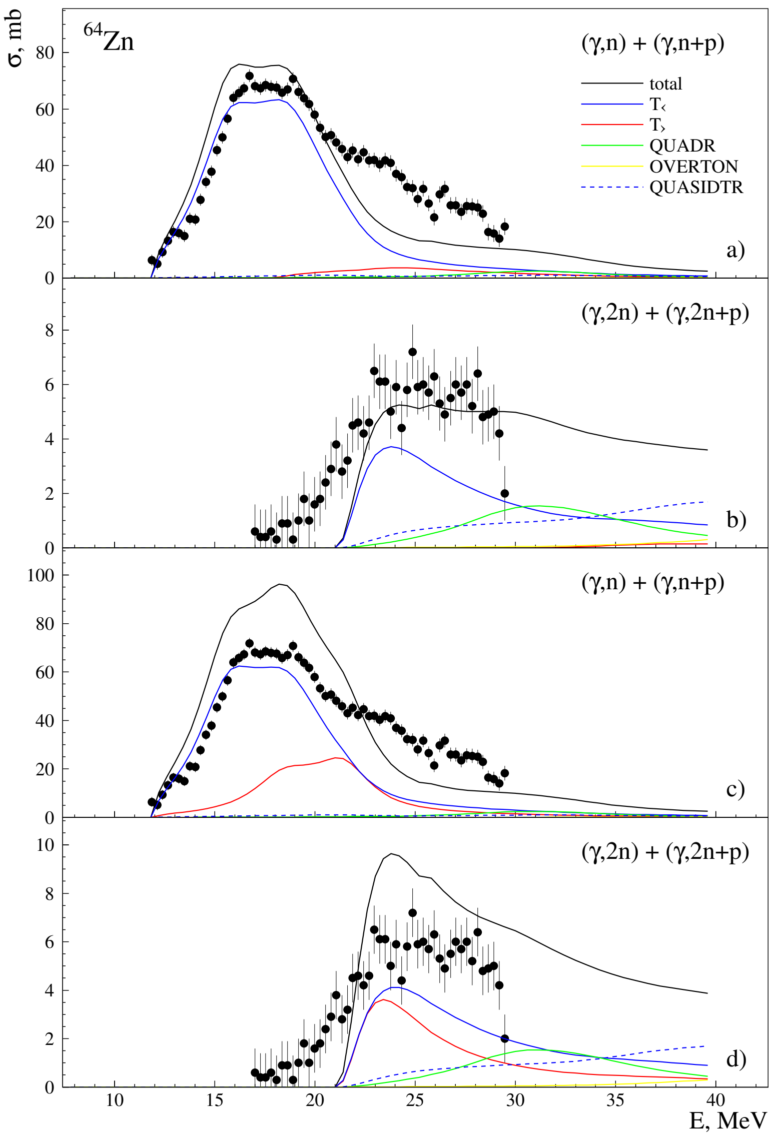

Figure 4: Comparison of experimental [38] and calculated photoneutron cross sections for the ^{64}Zn nucleus. In each panel of the figure, the black, blue, red, green, yellow, and dashed black curves correspond, respectively, to the total cross section, the contribution to it of the $T_<$ GDR component, the $T_>$ GDR component, the isovector quadrupole resonance, the GDR overtone, and the quasi-deuteron component of the cross section. The theoretical results presented in panels a) and b) take into account the collectivization of the input dipole state and the isospin selection rules during its decay (see the blue and red curves). Panels c) and d) show the calculation results without taking these effects into account.

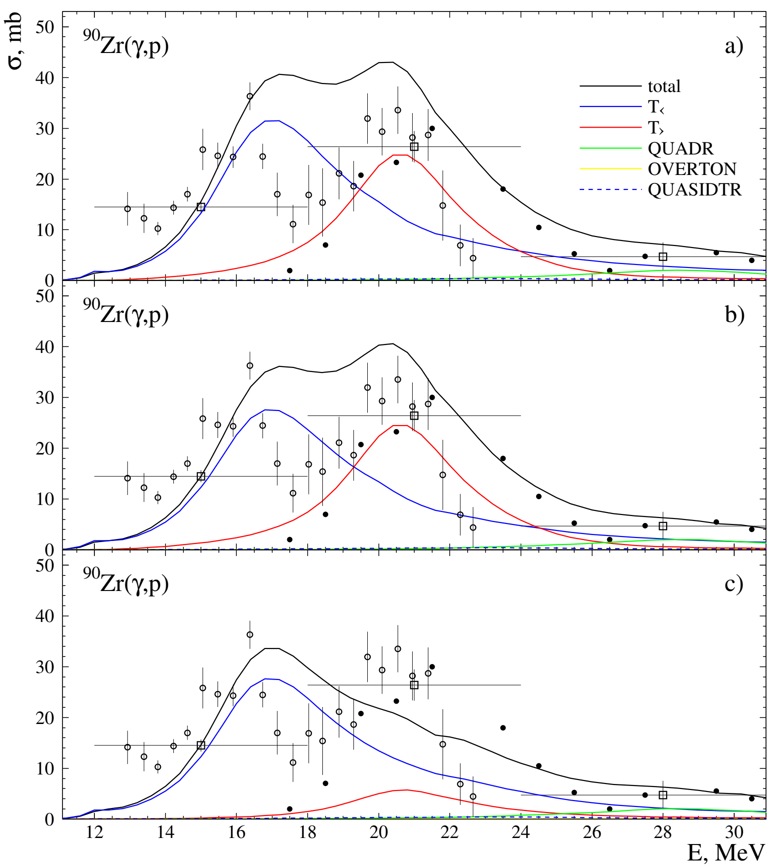

Figure 5: Comparison of experimental and calculated data for the cross section of the $^{90}\mathrm{Zr}(g,p)$ reaction. Experiment: open circles — [39], closed circles — [40], squares with horizontal errors — [41]. Theory: a) calculation taking into account isospin effects and collective properties of the doorway state for dipole excitation of the nucleus, b) without taking into account the collectivization of the doorway state, c) neither collectivization of the doorway state nor isospin effects are taken into account.

component of the GDR in ^{90}Zr will mainly decay, emitting a neutron, into low-lying states of the ^{89}Y nucleus.

For a full test of the importance of taking into account the effects under consideration when describing photonucleon reactions, it would, of course, also be desirable to compare the theoretical and experimental energy spectra of photonucleons, at least for one of the medium or medium-heavy nuclei. Unfortunately, we could not find the experimental information necessary for such a comparison in the sources available to us. Therefore, we will limit ourselves to considering how collective and isospin factors affect the theoretical energy spectrum of the total yield of photoprotons in the reaction $^{90}\mathrm{Zr}(g, px)$.

Figure 6 shows the energy spectra of photoprotons for this reaction, calculated: a) taking into account both isospin and collective effects during the decay of the GDR, b) taking into account only isospin effects, and c) without taking into account both effects under consideration. It is evident from the figure that, as expected, taking into account the collectivization of the doorway dipole state affects only the pre-equilibrium component of the energy spectrum, which increases significantly due to the emission of high-energy nucleons (quasi-direct photoeffect). Whereas taking into account isospin effects leads to a significant increase in the evaporation component of the photoproton spectrum due to the suppression of neutron emission during the decay of the $T_>$ component of the GDR.

In conclusion, we note that the CMPNR program was used by the staff of the Skobeltsyn Scientific Research Institute of Nuclear Physics of the Lomonosov Moscow State University (Centre for Photonuclear Experimets Data) to correct experimental photoneutron reaction data obtained using various methods of separating the yields of reactions of different multiplicities. This problem is discussed in the Appendix to this manual.

3. Installation and use of the CMPNR code

The CMPNR code is distributed in the form of Fortran 90 program source code. The program has been compiled and run using the GNU GFortran compiler (versions from 8 to 12) on Debian Linux 11 and 12 for the x86-64 architecture. On the Windows 10 x86-64 platform the Windows Subsystem for Linux emulation layer was used to compile and run CMPNR using GFortran 10. Other Unix-like environments with a recent GFortran version must be able to compile and run the CMPNR model.

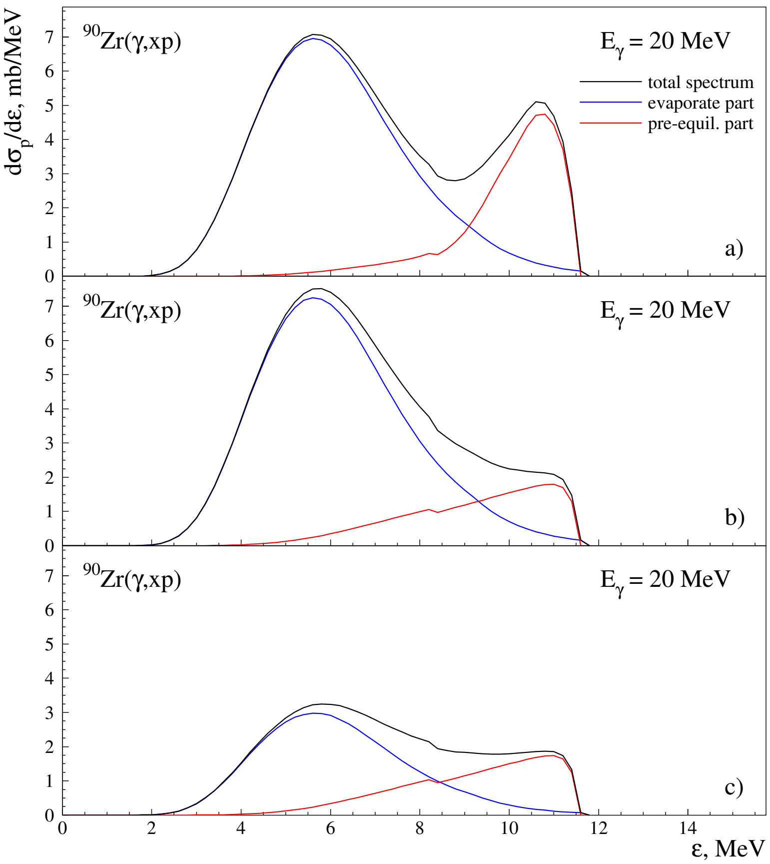

Figure 6: Effect of isospin selection rules and collectivization of the doorway dipole state on the energy spectrum of photoprotons emitted in the reaction $^{90}\mathrm{Zr}(\gamma, px)$. The panels of the figure show the results of calculations performed: a) taking into account both isospin effects and the collectivization effect for the dipole excitation of the nucleus, b) taking into account only isospin effects, and c) without taking into account both effects. The black curves describe the full spectrum, the blue ones its evaporation component, and the red ones the pre-equilibrium part of the spectrum.

CMPNR can be compiled by extracting the source code archive and executing the `make` command in the program's directory using the following terminal commands:

```
$ tar xzf kmfr-1.0.tar.gz
$ cd kmfr-1.0
$ make
```

The computation can be started by running the executable file `kmfr` with a configuration file in the Fortran namelist format. A sample configuration file is included in the archive:

```
!A sample configuration file for KMFR.
!Comments are denoted by '!'.
&kmfr_config
  element = 'Sm',
  mass_number = 154,
  deformation = 0.319,
  energy_max = 50,
  spectrum_energy = 20,
  density_model = 3,
  isospin_split_model = 2,
  qd_model = 1
/
```

In this file the following parameters are defined:

- `element` (string) and `mass_number` (integer) parameters are used to specify the target nucleus.
- `deformation` is the dimensionless quadrupole deformation parameter of the target nucleus.
- `energy_max` (in MeV units) specifies the energy range for calculation of the photonuclear reaction cross sections. The reaction cross sections are calculated from the reaction threshold to `energy_max`.
- `spectrum_energy` (in MeV units) specifies the energy of incident photons for which the spectrum of outgoing nucleons is calculated. If this parameter is not set or set to 0, the spectrum is not calculated.

- `density_model` (integer from 1 to 3) allows to specify the choice of the nuclear level density model. `density_model = 1` corresponds to the Constant Temperature model (CTM), `density_model = 2` corresponds to the Generalized Superfluid model (GSM), `density_model = 3` corresponds to the Back-shifted Fermi gas model (BFM).

- `isospin_split_model` (integer from 1 to 2) allows to specify the treatment of the isospin effects of the GDR decay. `isospin_split_model = 1` corresponds to the use of the Fallieros expressions, `isospin_split_model = 2` corresponds to the usage of the formalism of the semi-microscopic nuclear vibration model described in Section 2.3.

- `qd_model` (integer from 1 to 2) allows to specify whether to ignore (`qd_model = 1`) or consider (`qd_model = 2`) the collective correlations in the doorway dipole state.

With the included sample configuration file the program can run from the program directory using the following command:

```
$ ./kmfr < sample.cfg
```

Upon successful calculation an output subdirectory is created in the `data` directory whose name corresponds to the target nucleus. The calculated cross sections are tabulated in the `sct`i`.dat` files, where the index i corresponds to the specific partial reaction. The list of the partial reactions and corresponding values of i can be found in the `key` file. Each line of this file has the following format:

$$i \qquad \sigma_{\text{int}} \qquad B_i \qquad n_\pi \qquad n_\nu,$$

where i denotes the index of the partial reaction, σ_{int} is the energy-integrated cross section of this reaction in mb MeV units, B_i denotes the energy threshold of the reaction in MeV, and n_π and n_ν correspond to the number of outgoing protons and neutrons in the partial reaction, respectively. For each partial reaction the corresponding cross section in the `sct`i`.dat` file is represented as table with 7 columns:

- column 1: incident photon energy in MeV,

- column 2: total reaction cross section,

- column 3: contribution of the $T_<$ component of the GDR to the total cross section,
- column 4: contribution of the $T_>$ component of the GDR to the total cross section,
- column 5: contribution of the quadrupole giant resonance to the total cross section,
- column 6: contribution of the GDR overtone to the total cross section,
- column 7: contribution of the qausi-deutron photoabsorption mechanism to the total cross section.

All cross section values are specified in the mb units.

The `Spc_n.dat` and Spc_p.dat files contain the energy spectra of the outgoing neutrons and protons calculated at the incident photon energy `spectrum_energy` and integrated over the emission direction and reaction type. The format of these files is the following:

- column 1: incident photon energy,
- column 2: outgoing nucleon energy,
- column 3: total outgoing nucleon spectrum in mb/MeV units,
- column 4: contribution of the evaporation process to the total nucleon spectrum,
- column 5: contribution of the pre-equilibrium process to the total nucleon spectrum.

Appendix A. Using CMPNR to correct experimental data

The absolute majority of partial cross sections of photonucleon reactions was obtained in experiments used the beams of quasimonoenergetic annihilation photons performed at the Lawrence Livermore National Laboratory (USA) and the Centre d'Etudes Nucleaires de Saclay (France) [44, 45]. In both laboratories, neutrons were recorded after they had been slowed down, as a result of which the partial reactions $(\gamma, 1n)$, $(\gamma, 1n1p)$, $(\gamma, 1n2p)$, ... was taken into account in the total neutron yield once, the reactions $(\gamma, 2n)$, $(\gamma, 2n1p)$, ... — twice, the reactions $(\gamma, 3n)$, ... — three times, etc.

Measurements of the cross section of neutron yield, equal by definition

$$\sigma(\gamma, xn) = \sigma(\gamma, 1n) + \sigma(\gamma, 1n1p) + \sigma(\gamma, 1n2p) + 2\sigma(\gamma, 2n) + 2\sigma(\gamma, 2n1p) + 3\sigma(\gamma, 3n) + ..., \quad \text{(A.1)}$$

gave similar results in both laboratories. In the experiments under consideration, however, serious problems arise in measuring the cross-sections of specific partial reactions, since this requires sorting the registered neutrons into groups corresponding to a certain multiplicity of their emission from the target nucleus. Both at Saclay and at Livermore, in one form or another, an indirect method is used to determine the multiplicity of registered neutrons, based on the fact that with an increase in the number of neutrons emitted by a nucleus, their average energy is decreased. Unfortunately, this method of sorting neutrons by multiplicity does not completely solve the above-mentioned problem of measuring individual cross sections of partial reactions. In particular, the data obtained in Saclay and Livermore for the cross-sections of reactions $(\gamma, 1n)$ and $(\gamma, 2n)$ for many nuclei studied differ significantly (up to 100% in absolute value).

In Fig. A.7 for 19 nuclei the ratios of the integral cross sections ($R^{\text{int}}_{S/L} = R^{\text{int}}_{\text{Saclay/Livermore}}$) of the reactions $(\gamma, 1n)$ and $(\gamma, 2n)$ are given, calculated according to the data of Saclay and Livermore. As can be seen from the figure, the Saclay data for the reaction $(\gamma, 1n)$ systematically exceed the Livermore data ($\langle R^{\text{int}}_{S/L}(\gamma, 1n)\rangle = 1.08$) and are lower than these data ($\langle R^{\text{int}}_{S/L}(\gamma, 2n)\rangle = 0.83$) for the reaction $(\gamma, 2n)$).

Thus, the experimental methods used in practice do not allow for a reliable assessment of the cross-sections of partial photoneutron reactions. Therefore, it is necessary to make theoretical corrections to the experimental data obtained. This can be achieved [69] if the cross sections $\sigma(\gamma, \{in\dots\})$ of partial photoneutron reactions are divided into two factors, the first of which can be more or less satisfactorily calculated within the framework of existing semi-classical statistical models of photonucleon reactions, and the second can be estimated in the course of direct photoneutron measurements:

$$\sigma(\gamma, \{in\dots\}) = F_{\{in\dots\}}\sigma(\gamma, xn), \quad \text{(A.2)}$$

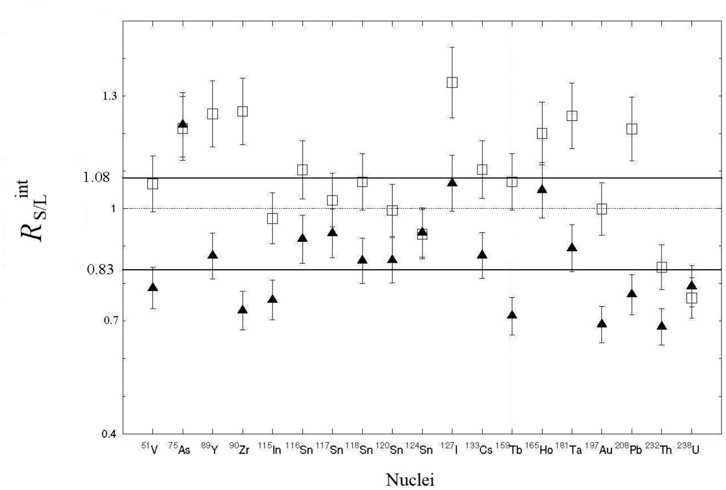

Figure A.7: The systematic of the ratios $R^{\rm int}_{S/L}(\gamma, 1n)$ (open squares) and $R^{\rm int}_{S/L}(\gamma, 2n)$ (closed triangles) according to data obtained in Saclay and Livermore experiments.

where

$$F_{\{in\ldots\}} = \sigma(\gamma, \{in\ldots\})/\sigma(\gamma, xn) = \\ \sigma(\gamma, in\ldots)/(\sigma(\gamma, 1n) + \sigma(\gamma, 1n1p) + \sigma(\gamma, 1n2p) \\ + 2\sigma(\gamma, 2n) + 2\sigma(\gamma, 2n1p) + 3\sigma(\gamma, 3n) + \ldots), \quad \text{(A.3)}$$

is the ratio of the cross-section $\sigma(\gamma, \{in\ldots\})$ of the partial photoneutron reaction to the cross-section $\sigma(\gamma, xn)$ of the total photoneutron yield (see (A.1)) and the indices $\{in\ldots\}$ takes the values 1n, 1n1p, 1n2p, ...; 2n, 2n1p,...; 3n, ...

Because one does not see [43] similar disagreements between total photoneutron reaction cross sections

$$\sigma(\gamma, sn) = \sigma(\gamma, 1n) + \sigma(\gamma, 2n) + \sigma(\gamma, 3n) + \ldots \quad \text{(A.4)}$$

and neutron yield cross sections

$$\sigma(\gamma, xn) = \sigma(\gamma, 1n) + 2\sigma(\gamma, 2n) + 3\sigma(\gamma, 3n) + \ldots \quad \text{(A.5)}$$

data obtained at both laboratories mean that systematic disagreements between partial reaction cross sections are because of definite shortcomings of the method of photoneutron multiplicity sorting used for partial reactions separation.

As can be seen from the relation (A.3), the values of $iF_{\{in\dots\}}$ characterize the relative probabilities of various partial photoneutron reactions $(\gamma, \{in\dots\})$. and satisfy the normalization condition

$$\sum_{\{in\dots\}} iF\{in\dots\} = 1. \tag{A.6}$$

It follows from this that the factors $F_{\{in\dots\}}$ are positive and should not exceed the values 1, 1/2, 1/3, ... for reactions with the emission of one ($i = 1$), two ($i = 2$), three ($i = 3$), etc. neutrons.

Competition of different photonucleon reactions is considered in all semi-classical statistical models of nuclear reactions (such as exciton, hybrid, and models included in the GNASH and TALYS codes). It is usually assumed that the photoabsorption cross section $\sigma_{\text{abs}}(E_\gamma)$ can be approximated by the sum of the Lorentz curves describing GDR and the quasi-deuteron photoabsorption cross section. A large number of calculations of photonucleon reactions have been performed using these models, which has made it possible to standardize the model parameters used to describe the evolution of a composite nuclear system formed after the absorption of a γ-quantum. It should be noted that all these models do not take into account the influence of isospin and collective effects on the decay properties of a composite system. As a result, the quality of the photoabsorption cross-section estimate does not actually affect the estimate of the theoretical factors $F^{\text{theor}}_{\{in\dots\}} = \sigma(\gamma, \{in\dots\})^{\text{theor}}/\sigma(\gamma, xn)^{\text{theor}}$, since under the assumptions made, both the numerator and denominator of fraction (A.3) will be proportional to $\sigma_{\text{abs}}(E_\gamma)$.

In the case of relatively heavy nuclei ($A > 100$), for which the influence of isospin and collective effects on the decay characteristics of the composite system is relatively small, such an approximation of the $F_{\{in\dots\}}$ factors seem quite acceptable. However, when calculating $F^{\text{theor}}_{\{in\dots\}}$ in lighter nuclei ($A \leq 60$), these effects cannot be ignored, since this will lead to an underestimation of the proton yield compared to the neutron yield. Therefore, in the works [Varlamov et al.] it is proposed to use the CMPNR program when calculating the factors $F^{\text{theor}}_{\{in\dots\}}$, taking into account the role of isospin and collective effects both in the formation and in the decay of the composite state.

Like the true values of $F_{\{in\dots\}}$, the theoretical estimates of $F^{\text{theor}}_{\{in\dots\}}$ are positive, satisfy the normalization condition (A.6) and do not exceed the limit values. At the same time, for the factors $F^{\text{exp}}_{\{in\dots\}} = \sigma(\gamma, \{in\dots\})^{\text{exp}}/\sigma(\gamma, xn)^{\text{exp}}$, all three conditions listed above may be violated, since when measuring $\sigma(\gamma, \{in\dots\})^{\rm exp}$, an incorrect method for separating photoneutron reactions of different multiplicities is used.

This is illustrated in Fig. A.8, which shows the dependence of the values of $F_i^{\rm exp}$ and $F_i^{\rm theor}$ (CMPNR calculation) for reactions with the emission of $i = 1, 2$ neutrons from the nuclei of ^{65}Cu, ^{116}Sn and $i = 1, 2, 3$ neutrons from the nucleus of ^{94}Zr.

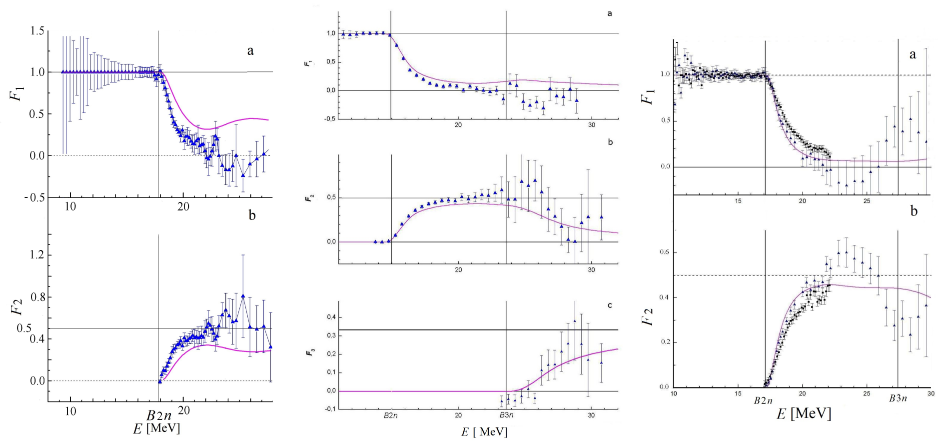

Figure A.8: The comparisons of the ratios $F_i^{\rm exp}$ (Livermore– triangles, Saclay – squares) and $F_i^{\rm theor}$ (CMPNR – curves) obtained for ^{65}Cu [49, 50], ^{94}Zr [51, 52], and ^{116}Sn [53, 54, 55]: (a) F_1, (b) F_2, and (c) F_3.

The correction of the experimental partial cross sections $\sigma(\gamma, \{in\dots\})^{\rm exp}$, as noted above, can be performed using relation (A.2), in which the factor $F_{\{in\dots\}}$ is estimated theoretically, and the cross section $\sigma(\gamma, xn)$ is extracted directly from the experiment. As a result, we obtain the following formula for calculating the evaluated (corrected) values of the partial photoneutron cross sections [69]:

$$\sigma(\gamma, \{in\dots\})^{\rm eval} = F_{\{in\dots\}}^{\rm theor} \sigma(\gamma, xn)^{\rm exp}, \quad \text{(A.7)}$$

where $F_{\{in\dots\}}^{\rm theor} = \sigma(\gamma, in\dots)^{\rm theor}/\sigma(\gamma, xn)^{\rm theor}$ is the theoretical estimate of the factor $F_{\{in\dots\}}$ within the framework of CMPNR and $\sigma(\gamma, xn)^{\rm exp}$ is the experimental neutron yield cross-section.

Note that, since the values of $F_{\{in\dots\}}^{\rm theor}$ obey the normalization condition (A.6), the evaluated partial cross sections $F_{\{in\dots\}}^{\rm theor}$, in contrast to the experimental cross sections $\sigma(\gamma, \{in\dots\})^{\rm exp}$, meet the condition

$$\sum_{\{in\dots\}} i\sigma(\gamma, \{in\dots\})^{\rm eval} = \sigma(\gamma, xn)^{\rm exp}. \tag{A.8}$$

Figure A.9 shows the experimental neutron yield cross sections $\sigma(\gamma, xn)^{\rm exp}$ obtained at Saclay and Livermore for the nuclei ^{65}Cu, ^{115}In and ^{159}Tb, and also a comparison is made between the partial cross sections $\sigma(\gamma, in)^{\rm eval}$ and $\sigma(\gamma, in)^{\rm exp}$ for these nuclei.

The ambiguity of the experimental data presented in Fig. A.9 is due to significant shortcomings of the experimental method of separating the yields of partial reactions of different multiplicities, based on sorting the registered neutrons by energy. The fact is that the energy ranges of neutrons emitted in different partial reactions overlap, since the nucleus after the emission of a neutron can remain not only in the ground state, but also in an excited state. This leads to the fact that, depending on the features of the neutron detectors used in the measurements, the cross section of a particular partial reaction can be overestimated due to other photoneutron reactions. Thus, in Livermore's data, the cross section of the reaction $\sigma(\gamma, 1n)$ is overestimated with a simultaneous decrease in the cross section of the reaction $\sigma(\gamma, 2n)$, while in Saclay's data, on the contrary, the cross section of the reaction $\sigma(\gamma, 2n)$ is overestimated due to the cross section of the reaction $\sigma(\gamma, 1n)$. In a number of cases (^{181}Ta, ^{197}Au and ^{209}Bi), the unreliability of the photoneutron reaction cross sections obtained using the method of separating the yields of partial reactions of different multiplicities was confirmed by comparing the newly evaluated data with the results obtained in activation experiments (see, for example, [56, 57, 66, 67, 68]), in which de-excitation gamma spectra corresponding to specific final nuclei are studied, which allows direct and reliable evaluation of the yields of various partial photonucleon reactions.

In conclusion, it should be emphasized that the success or failure of using the above procedure for correcting experimental photoneutron data depends on the global characteristics of the nuclei to which it is applied. Good results can be expected for β-stable medium and heavy nuclei with a pseudo-rigid surface, since the CMPNR program was developed precisely for such nuclei.

References

[1] J.M. Laget, Nucl. Phys. **A 312**, 265 (1978).

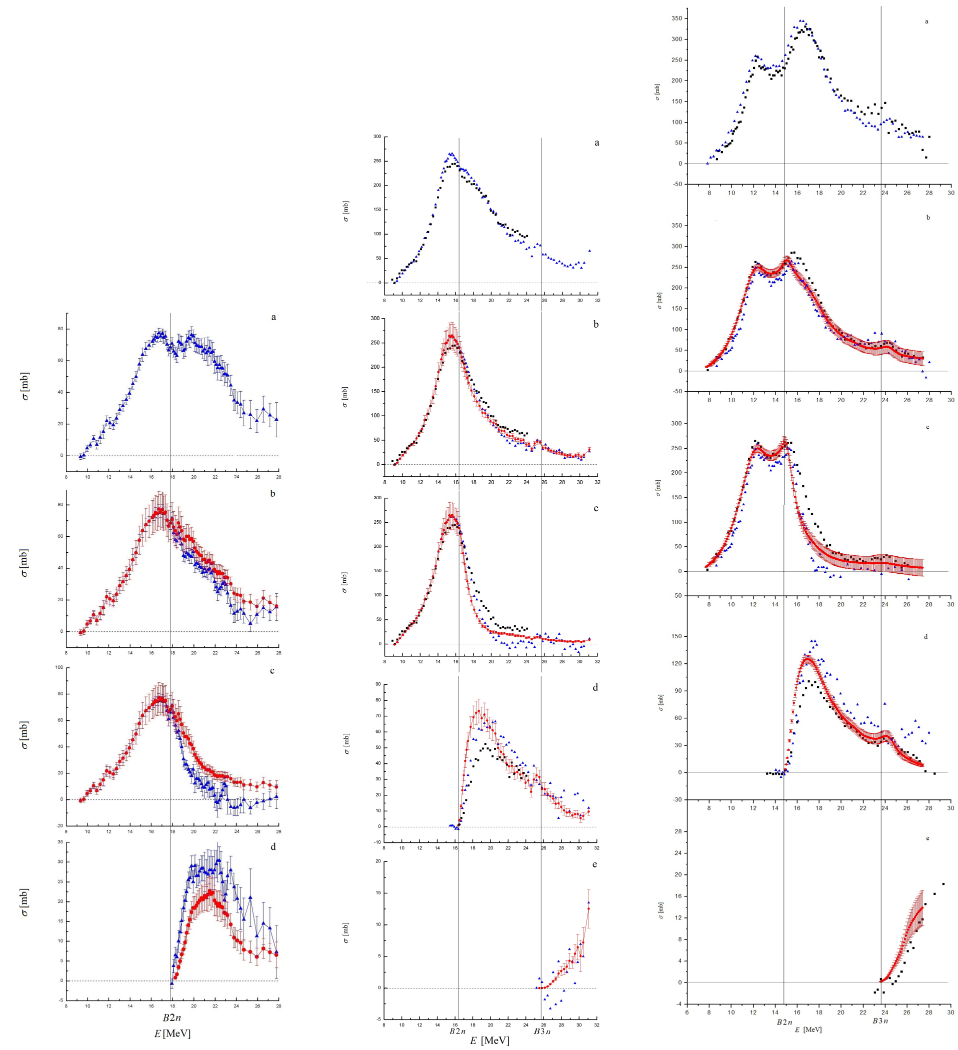

Figure A.9: The comparisons of the experimental cross sections (Livermore – triangles, Saclay – squares) and evaluated ones (circles) in the cases of ^{65}Cu [49, 50], ^{115}In [55, 65], and ^{159}Tb [53, 70, 71] for various reactions: (a) $\sigma(\gamma, xn)$, (b) $\sigma(\gamma, sn)$, (c) $\sigma(\gamma, 1n)$, (d) $\sigma(\gamma, 2n)$, (e) $\sigma(\gamma, 3n)$.

[2] J. M. Laget, *Lecture Notes in Physics*, Vol. **137**, edited by H. Arenhovel and A. M. Saruis (Springer-Verlag, Berlin, 1981), p. 148.

[3] G.E. Brown, Unified Theory of NuclearModels and Forces (North-Holland, Amsterdam, 1967; Atomizdat, Moscow, 1970).

[4] A. B. Migdal, Theory of Finite Fermi Systems and Applications to Atomic Nuclei (Nauka, Moscow, 1983, 2nd ed.; Interscience, New York, 1967, transl. 1st ed.).

[5] B. Buck and A. D. Hill, Nucl. Phys. **A 95**, 271 (1967).

[6] S. Kamerdzhiev et al., Nucl. Phys. **A 555**, 90 (1993).

[7] S.P. Kamerdzhiev et al., Phys. Part. Nucl. **28**, 134 (1997).

[8] A. Rodin and M.H. Urin, Phys. Rev. **C 66**, 064608 (2002).

[9] O. Bohr and B.R. Mottelson, Nuclear Structure, vol. 2: Nuclear Deformations, (Benjamin, New York, 1975; Mir,Moscow, 1977).

[10] B.S. Ishkhanov and V.N. Orlin, Phys. Part. Nucl. **38**, 232 (2007).

[11] J.S. Levinger, Phys. Rev. 84, 43 (1951); Phys. Lett. **B 82**, 181 (1979).

[12] M.B. Chadwick et al., Phys. Rev. **C 44**, 814 (1991).

[13] C.K. Cline and M. Blann, Nucl. Phys. **A 172**, 225 (1971).

[14] C. K. Cline, Nucl. Phys. **A 210**, 590 (1973).

[15] E. Gadioli, E. Gadioli Erba, and P.G. Sona, Nucl. Phys. **A 217**, 589 (1973).

[16] J. Dobes and E. Betak, Nucl. Phys. **A 272**, 353 (1976).

[17] M. Blann and H. K. Vonach, Phys. Rev. **C 28**, 1475 (1983).

[18] M. Blann, Phys. Rev. **C 54**, 1341 (1996).

[19] M. Blann and M.B. Chadwick, Phys. Rev. **C 57**, 233 (1998)

[20] H. Feshbach, A. Kerman, and S. Koonin, Ann. Phys. (N. Y.) **125**, 429 (1980).

[21] H. Nishioka, H.A. Weidenmuller and S. Yoshida, Ann. Phys. (N. Y.) **183**, 166 (1988).

[22] A.J. Koning and M.B. Chadwick, Phys. Rev. **C 56**, 970 (1997).

[23] B.S. Ishkhanov and V.N. Orlin, Phys. At. Nucl. **74**, 19 (2011).

[24] B.S. Ishkhanov and V.N. Orlin, Phys. At. Nucl. **76**, 30 (2013).

[25] B.S. Ishkhanov and V.N. Orlin, Phys. At. Nucl. **78**, 557 (2015).

[26] S. Fallieros and B. Goulard, Nucl. Phys. **A 147**, 593 (1970).

[27] R. O. Akyuz and S. Fallieros, Phys. Rev. Lett. **27**, 1016. (1971).

[28] M. Danos, Nucl. Phys. **A 5**, 23 (1958).

[29] K. Okamoto, Prog. Theor. Phys. **15**, 75 (1956).

[30] M. Goldhaber and S. Teller, Phys. Rev. **74**, 1046 (1948).

[31] H. Steiwedel et al., Phys. Rev. **79**, 1019 (1950).

[32] B.S. Ishkhanov and V.N. Orlin, Phys. At. Nucl. **66**, 659 (2003).

[33] B.S. Ishkhanov and V.N. Orlin, Phys. At. Nucl. **71**, 493 (2008).

[34] A.J. Koning, S. Hilaire and S. Goriely, Nucl Phys. **A 810**, 13 (2008).

[35] J. Kopecky and M. Uhl, Phys. Rev. **C 41**, 1941 (1990).

[36] A. Gilbert and A.G.W. Cameron, Can. J. Phys. **43**, 1446 (1965).

[37] B.S. Ishkhanov and V.N. Orlin, Phys. At. Nucl. **72**, 410 (2009).

[38] P. Carlos et al., Nucl. Phys. **A 258**, 365 (1976).

[39] D. Brajnik et al., Phys. Rev. **C 13**, 1852 (1976).

[40] И.И. Душков и др., Изв. АН СССР **29**, 213 (1965).

[41] W.R. Dodge et al., Phys. Rev. **C 32**, 781 (1985).

[42] B.S. Ishkhanov, I.M. Kapitonov. Interaction of electromagnetic radiation with atomic nuclei. Izdsatel'stvo Moskovskogo Universiteta, Moscow, Russia. 1979.

[43] V.V. Varlamov, B.S. Ishkhanov. Study of consistency between (γ, xn), $[(\gamma, 1n) + (\gamma, 1n1p)]$, and $(\gamma, 2n)$ reaction cross sections using data systematics. IAEA Tech Rep. INDC(CCP)–432, IAEA. 2002.

[44] S.S. Dietrich, B.L. Berman. At. Data Nucl. Data Tables 38 (1988) 199.

[45] IAEA Nuclear Data Section database "EXFOR. Experimental nuclear reaction data", http://www-nds.iaea.org/exfor.

[46] E. Wolynec, A.R.V. Martinez, P. Gouffon, Y. Miyao, V.A. Serrao, M.N. Martins. Phys. Rev. 29 (3) (1984) 1137.

[47] V.V. Varlamov, B.S. Ishkhanov, V.N. Orlin, S.Yu. Troshchiev. Bull. Rus. Acad. Sci. Phys. 74 (6) (2010) 842.

[48] V.V. Varlamov, B.S. Ishkhanov, V.N. Orlin, V.A. Chetvertkova. Bull. Rus. Acad. Sci. 74 (6) (2010) 883.

[49] V.V. Varlamov, A.I. Davydov, M.A. Makarov, В.Н. Орлин, Н.Н. Песков. Bull. Rus. Acad. Sci. Phys. 80 (3) (2016) 317.

[50] S.C. Fultz, R.L. Bramblett, J.T. Caldwell, R.R. Harvey. Phys. Rev. 133 (1964) B1149.

[51] V.V. Varlamov, M.A. Makarov, N.N. Peskov, M.E. Stepanov. Phys. Atom. Nucl. 78 (5) (2015) 634.

[52] B.L. Berman, J.T .Caldwell, R.R. Harvey, M.A. Kelly, R.L. Bramblett, S.C. Fultz. Phys.Rev. 162, 1098 (1967).

[53] V.V. Varlamov, B.S. Ishkhanov, V.N. Orlin. Phys. Atom. Nucl. 75 (11) (2012) 1339.

[54] S.C. Fultz, B.L. Berman, J.T. Caldwell, R.L. Bramblett, M.A. Kelly. Phys. Rev. 186 (4) (1969) 1255.

[55] A. Lepretre, H. Beil, R. Bergere, P. Carlos, A. De Miniac, A. Veyssiere, K. Kernbach. Nucl. Phys. A 219 (1974) 39.

[56] V.V. Varlamov, B.S. Ishkhanov, V.N. Orlin, K.A. Stopani, Eur. Phys. J. A 50 (2014) 114.

[57] S.S. Belyshev, D.M. Filipescu, I. Gheoghe, B.S. Ishkhanov, V.V. Khankin, A.S. Kurilik, A.A. Kuznetsov, V.N. Orlin, N.N. Peskov, K.A. Stopani, O. Tesileanu, V.V. Varlamov. Eur. Phys. J. A 51 (2015) 67.

[58] V.V.Varlamov, B.S.Ishkhanov, V.N.Orlin, N.N.Peskov. Phys. Atom. Nucl. 79, N 4 (2016) 501.

[59] V.V. Varlamov, A.I. Davydov, B.S. Ishkhanov, Eur. Phys. J. A 53 (2017) 180.

[60] V.V. Varlamov, A.I. Davydov, B.S. Ishkhanov, V.N. Orlin, Eur. Phys. J. A 54 (2018) 74.

[61] V. Varlamov, A. Davydov, V. Kaidarova, V. Orlin, Phys. Rev. C 99 (2) (2019) 024608.

[62] V.V. Varlamov, A.I. Davydov, V.N. Orlin, Amer. J. Phys. Appl. 8 (5) (2020) 64.

[63] V.V. Varlamov, A.I. Davydov, V.N. Orlin, Eur. Phys. J. A. 57(10) (2021) 287.

[64] V.V. Varlamov, A.I. Davydov, V.N. Orlin, Eur. Phys. J. A 58 (2022) 123.

[65] V.V. Varlamov, V.N. Orlin, N.N. Peskov, M.E. Stepanov. Bull. Rus. Acad. Sci. Phys. 77 (4) (2013) 388.

[66] V.V. Varlamov, B.S. Ishkhanov, V.N. Orlin, N.N. Peskov, M.E. Stepanov. Phys. Atom. Nucl. 76 (4) (2013) 1403.

[67] V.V. Varlamov, B.S. Ishkhanov, V.N. Orlin. Phys. Rev. C 96 (4) (2017) 044606.

[68] B.S. Ishkhanov, V.N. Orlin, S.Yu. Troshchiev. Phys. Atom. Nucl. 75 (3) (2012) 253.

[69] V.V. Varlamov, A.I. Davydov, V.N. Orlin. Atom. Data Nucl. Data Tables. 161 (2025) 101697.

[70] R. L. Bramblett, J. T. Caldwell, R. R. Harvey, S. C. Fultz. Phys. Rev. 133 (1964) B869.

[71] R. Bergere, H. Beil, A. Veyssiere. Nucl. Phys. A 121 (1968) 463.

[72] B.L. Berman, D.D. Faul, R.A. Alvarez, P. Meyer, D.L. Olson, Phys. Rev C. 19 (4) (1979) 1205.

[73] V.V. Varlamov, A.I. Davydov, I.A. Mostakov. Eur. Phys. J. A. 60 (2024) 44.

[74] V.V. Varlamov, A.I. Davydov, I.A. Mostakov, V.N. Orlin. Phys. Atom. Nucl. 87, N6 (2024) 669.

[75] V.V. Varlamov, A.I. Davydov, I.A. Mostakov, V.N. Orlin. Phys. Atom. Nucl. 86, N 5 (2023) 600.

[76] V.V. Varlamov, A.I. Davydov, V.N. Orlin. Phys. Atom. Nucl. 85, N 4 (2022) 316.

[77] V.V. Varlamov, A.I. Davydov, V.N. Orlin. Phys. Atom. Nucl. 85, N 5 (2022) 411.

[78] V.V. Varlamov, A.I. Davydov, V.N. Orlin. Eur. Phys. J. A, 58 (2022) 123.

[79] V.V. Varlamov, A.I. Davydov, V.N. Orlin. Bull. Rus. Acad. Sci. Phys., 87, N 8 (2023) 1188.

[80] V.V. Varlamov, A.I. Davydov, I.A. Mostakov. Bull. Rus. Acad. Sci. Phys., 88, N 8 (2024) 1211.

[81] B.I. Goryachev, B.S. Ishkhanov, I.M. Kapitonov, I.M. Piskarev, B.G. Shevchenko, O.P. Shevchenko. Sov. J. Nucl. Phys. 11 (1970) 141.

[82] S. C. Fultz, R. A. Alvarez, B. L. Berman, P. Meyer, Phys. Rev. C 10 8 (1974) 60.

[83] J.M. Blat and V.F. Weisskopf. Theoretical Nuclear Physics. (J.Wiley and Sons, Inc. New York, 1952).